ISSN(Online) : 2319-8753
ISSN (Print) : 2347-6710

International Journal of Innovative Research in Science, Engineering and Technology

(An ISO 3297: 2007 Certified Organization)

Website: www.ijirset.com

Vol. 6, Issue 6, June 2017

Effect on and Correlation between Particle Size, Lattice Constant and AC Conductivity of Nanocrystalline spinel Ferrite Material due to substitution of Ni^{2+}, Co^{2+} and Cu^{2+} in CuCo, NiCu and CoNi Respectively Prepared by Sol Gel Auto Combustion Method

A.M. Tamboli[1*], Dr. Mazahar Farooqi[3], Dr. J. M. Pathan[4], Dr. Gulam Rabbani[2]

Associate Professor, Department of Electronic Science, Poona College, Pune, Maharashtra, India[1]

Associate Professor, Department of Physics and Electronics, Maulana Azad College, Aurangabad, Maharashtra, India[2, 4]

Associate Professor, Department of Chemistry, Dr. Rafiq Zakaria College for Women, Navkhanda, Aurangabad, Maharashtra, India[3]

ABSTRACT: Herein the preparation of ferrite materials by using chemical reactions such as SOL-GEL Auto Combustion Technique is explained and importance of Nanocrystalline spinel ferrite material. Structural characterization of the annealed samples at 400˚C for 4 hours was done by using X-ray diffraction method (XRD). The single phase formation of $NiCuCoFe_2O_4$ was confirmed by X-ray diffraction analysis. The Fourier transfor Infra Red Spectra (FT-IR) confirmed that the synthesized material is ferrite. XRD revealed that the average crystalline particle size which was calculated by using Scherer method is between 22 to 32 nm. The lattice constant is also calculated. The pellets are made from ferrite powder by using polyvinyl alcohol (PVA) as binder. The data obtained from LCR-Q meter is used for calculating Dielectric loss tangent (tan δ), Dielectric constant (έ) and AC Conductivity in the frequency range of 100Hz to 5MHz at room temperature. The effect on Particle size is observed due to doping of Ni^{2+} , Co^{2+} and Cu^{2+} in CuCo, NiCu and CoNi respectively .The correlation ship between the Particle size, lattice constant and AC Conductivity is explained.

KEYWORDS: Sol-gel auto-combustion, X-ray diffraction (XRD), FT-IR, LCR-Q meter.

I. INTRODUCTION

Nanocrystalline Materials have become a subject of considerable interest in last few decades and many physical studies have been devoted to them. The ability to produce nanosized due to small grain size which changes the magnetic, dielectric and resistivity properties and opened new application for materials such as magnetic data storage, strong magnetron in electronics, Ferro fluid technology, magnetically targeted drug carriers, filters in electronic communication and agents in magnetic resonance imaging.

Nano-ferrites form an important class of Nanocrystalline materials because of their low weigh, high resistivity and low energy losses (eddy current) and hence have vast technological application over wide range of frequencies

ISSN(Online) : 2319-8753
ISSN (Print) : 2347-6710

International Journal of Innovative Research in Science, Engineering and Technology

(An ISO 3297: 2007 Certified Organization)

Website: www.ijirset.com

Vol. 6, Issue 6, June 2017

[1-2]. Recent studies have shown that the physical properties of nanoparticles are influenced significantly by the processing technique [3-4]. Since crystallite size, distribution of particle sizes and inter particle spacing have the greatest impact on AC conductivity and Dielectric properties. Many wet-chemical methods are employed for the preparation of the nano-sized spinel ferrite. One of them is sol-gel auto combustion which has recently become very popular technique. It is a simple process, which offers significant saving in time and energy consumption over the traditional methods and requires a low sintering temperature. This method is used to obtain improved properties, more homogeneity and narrow particle distribution thereby influencing structural, electrical and Dielectric properties of spinel ferrite [5-7]. It is well known that, some magnetic properties such as saturation magnetization and Coercivity and some Dielectric properties such as Dielectric loss tangent (tan δ) , AC electrical conductivity (σ_{ac}) and Dielectric constant (Real Part= έ) depend strongly on the particle size and microstructure of the materials. Therefore, it is interesting and important to develop techniques by which the size and shape of the particles can be well controlled. One of the ways to prepare the nanocrystalline spinel ferrite material with required properties is Sol-gel auto combustion technique. In the present work we have systematically studied the effect of doping of Ni $^{2+}$, Co^{2+} and Cu^{2+} in CuCo, NiCu and CoNi respectively on structural properties and AC conductivity of Nanocrystalline spinel ferrite material.

II. RELATED WORK

2.1. Experimental technique

The high purity AR grade ferric nitrate ($Fe(NO_3)_3.9H_2O$), Copper nitrate ($Cu(NO_3)_2{\cdot}6H_2O$), Nickel nitrate ($Ni(NO_3)_2{\cdot}6H_2O$),Cobalt nitrate($Co(NO_3)_2{\cdot}6H_2O$), citric acid ($C_6H_8O_7$), ammonium hydroxide solution (NH_4OH) were used to prepare $Ni_{\ x}Cu_{\ 0.2}\ Co_{\ 0.8-x}\ Fe_2O_4$ nanoparticles by sol-gel auto combustion synthesis technique. In this chemical process Citric acid was used as a Fuel [8-10]. These nitrates and citric acid were weighed accurately to have proper stoichiometric proportion required in the final product. The mixed solutions of all the chemicals were stirred until the homogeneous solution is obtained. During the stirring process ammonium hydroxide solution was added drop by drop to obtain pH of 7. The mixed solution was simultaneously heated at 100 $^{\circ}$C for 3 to 4 h to form sol. The transparent sol was further heated at 100°C for 2 h for removal of water. The sol turns into a viscous brown gel. The temperature of the gel was further increased up to 120 $^{\circ}$C, after some time combustion of the gel takes place and fine powder of ferrite nanoparticles was obtained. The ferrite powder was sintered at 400°C for 4 hours in air medium to get better crystallization and homogeneous distribution in the spinel and finally ground to get $[(Ni_{.0.2}\ Cu_{.0.2}Co_{0.6})Fe_2O_4]$, $[(Ni_{.0.4}\ Cu_{.0.2}Co_{0.4})Fe_2O_4]$, $[(Ni_{.0.6}\ Cu_{.0.2}Co_{0.2})Fe_2O_4]$, $[(Ni_{.0.2}\ Cu_{.0.6}Co_{0.2})Fe_2O_4]$, $[(Ni_{.0.2}\ Cu_{.0.4}Co_{0.4})Fe_2O_4]$and $[(Ni_{.0.4}\ Cu_{.0.4}Co_{0.2})Fe_2O_4]$ ferrite powders. **Table 1** indicates Label and composition of ferrite materials for all six fractions divided in to three Sets.

The elemental stoichiometric coefficient, φ_e, is used to control the ratio of fuel to oxidizer in the reaction. φ_e represents the ratio between the oxidizing and reducing components of the metal nitrate fuel mixture. When φ_e is less than one ($\varphi_e<1$) it is fuel rich and when φ_e is greater than one ($\varphi_e>1$), the mixture does not have enough fuel for the completion of reaction. **Fig. 1** shows the flow chart of auto combustion synthesis used for the preparation of the ferrite powders and pellet.

2.2. Perpetration and Sintering of pellets

The pellets are prepared by mixing the polyvinyl alcohol (PVA) as binder in to ferrite powder. The mixed powder was uniaxially pressed by using a hydraulic press machine by applying the pressure of about 60 kg/cm^3 for about 1 minute in a die of 10mm diameter. The final sintering of pellets was carried out at 200^{o}C for about 2 hours in air medium to densify the pellets. The pellets of diameter D_o-10 mm, thickness-2 mm are fabricated. The prepared samples of pellets were sintered in a furnace which uses electricity for heating the chamber with the help of super kanthal ($MoSi_2$) heating elements and alumina insulation boards as chamber walls. The dimension of chamber is 250x150x150 mm. The thermal regime of the furnace was controlled through a “Eurotherm” programmer-cum-controller designed by using microcontroller with an accuracy of ± 2°C. The compacted samples heated from room temperature to 200^{o}C at a rate 1^{o}C/min followed by a soaking at 200^{o}C for 2 hours for binder burnout.

ISSN(Online) : 2319-8753
ISSN (Print) : 2347-6710

International Journal of Innovative Research in Science, Engineering and Technology

(An ISO 3297: 2007 Certified Organization)

Website: www.ijirset.com

Vol. 6, Issue 6, June 2017

2.3. Characterization of AC conductivity (σ_{ac})

The **AC** conductivity (σ_{ac}) of prepared samples was measured in the frequency range of 100 Hz to 5 MHz by using impedance analyser (LCR-Q Meter) meter at room temperature. The data acquisition system of digital impedance analyser (LCR-Q meter) provides the information of applied frequency (f), measured Series Capacitance (Cs), Parallel Capacitance (Cp), Quality factor (Q).

The data provided by digital impedance analyser meter and by using the thickness of pellet, d=0.002 meter, Diameter of pellet= 10 millimetre the Area of pellet = πr^2 = 3.14*.005*.005 meter^2=0.0000785 meter^2 is calculated and it is used for calculations of AC Conductivity (σ_{ac}) after calculating real part of dielectric constant (**ε'**), dielectric loss tangent (tan δ). Following equations are used

$$\text{Dielectric loss tangent} = (\tan\delta) = 1/Q = \varepsilon'' / \varepsilon' \quad -(1)$$

$$\text{Dielectric constant (Real Part)} = \acute{\varepsilon} = Cp*d/\varepsilon_0*A \quad -(2)$$

$$\text{Dielectric constant (Imaginary Part)} = \varepsilon'' = (\tan\delta)* \varepsilon' \quad -(3)$$

$$\text{AC electrical conductivity} = \boldsymbol{\sigma_{ac}} = 2\pi f * \varepsilon_0 * \varepsilon' * (\tan\delta) = \omega * \varepsilon_0 * \varepsilon' * (\tan\delta) \quad -(4)$$

$$\text{Lattices Constant (Å) is calculated by using the formula } \frac{1}{d^2} = \frac{1}{a^2 \times (h^2 + k^2 + l^2)} \quad -(5)$$

Table 2 shows average AC Conductivity for all six samples ferrite material calculated in the frequency range of 100Hz to 5MHz at room temperature.

III. RESULTS AND DISCUSSION

3.1. X-ray diffraction pattern

Fig. 2 shows the X-ray diffraction pattern of SET-II (D, E & A), $Ni_{0.2}\ Cu_{0.8-x}\ Co_x\ Fe_2O_4$ for x = 0.2, 0.4 and 0.6. All the compositions exhibit single phase cubic spinel structure with Fd_3m space group and exclude the presence of any secondary phase. All the reflections are slightly broader and less intense which indicate the nanocrystalline nature of the samples. The analysis of X-ray diffraction pattern revealed that all the samples under investigation possess single phase cubic spinel structure. Using the XRD data, the interplaner spacing 'd' values for all the reflections were determined using Bragg's law. The values of Particle size and lattice constant obtained from XRD data for all samples A to F of ferrite materials are given in **Table 3**.

3.2. Effect of Ni^{2+} substitution on Lattice constant and Particle size

In Set-I, It is observed that due to the concentration of Ni^{2+} ions in place of Co^{2+} ions the Bragg's angle shifts towards higher angle and thereby interplaner spacing 'd' values decreases. The lattice constant is found to decrease with increase in Ni^{2+} concentration x. The variations in lattice constant as a function of Nickel concentration x can be understood on the basis of the ionic radius of the substituted cations. Since the ionic radius of Ni^{2+} ions (0.69Å) is less than that of Co^{2+} ions (0.72Å), the substitution is expected to decrease the lattice constant with increase in Ni^{2+} concentration x . When the smaller nickel ions enters the lattice unit cell expands while preserving overall symmetry this is true as long as the lattice constant decreases with substituent concentration. The values of Particle size and lattice constant obtained from XRD data by varying Ni^{2+} doping are given in Table 4. It can be seen from **Table 4.**that, the lattice constant decreases with Ni^{2+} doping and obeys Vegard's law [11-14].The Particle size also decreases with Ni^{2+} doping. **Fig 3** and **Fig 4** show the correlation between Particle Size and Average AC Conductivity due to doping of Ni^{+2} respectively. **Fig 5** and **Fig 6** show the correlation between Lattice Constant and Average AC Conductivity due to doping of Ni^{+2} respectively.

3.3. Effect of Co^{2+} substitution on Lattice constant and Particle size

In Set-II, It is observed that due to the inclusion of Co^{2+} ions in place of Cu^{2+} ions the Bragg's angle shifts towards lower angle and thereby interplaner spacing 'd' values increases. The lattice constant is found to increase with

ISSN(Online) : 2319-8753
ISSN (Print) : 2347-6710

International Journal of Innovative Research in Science, Engineering and Technology

(An ISO 3297: 2007 Certified Organization)

Website: www.ijirset.com

Vol. 6, Issue 6, June 2017

increase in Co^{2+} concentration x. The variations in lattice constant as a function of Cobalt ions concentration x can be understood on the basis of the ionic radius of the substituted cations. Since the ionic radius of Co^{2+} ions (0.745Å) is greater than that of Cu^{2+} ions (0.73Å), the substitution is expected to increase the lattice constant with increase in Cobalt doping x**[15-17]**. The values of Particle size and lattice constant obtained from XRD data by varying Co^{2+} ions doping are given in **Table 5**. **Fig 7** and **Fig 8** show the correlation between Particle Size and Average AC Conductivity due to doping of Co^{2+} respectively. **Fig 9** and **Fig 10** show the correlation between Lattice Constant and Average AC Conductivity due to doping of Co^{2+} respectively.

When the larger Cobalt ions enters, the lattice unit cell expands while preserving overall symmetry this is true as long as the lattice constant increases with substituent concentration of Cobalt**[18-19]**.

3.4. Effect of Cu^{2+} substitution on Lattice constant and Particle size

In Set – III, It is observed that due to the inclusion of Cu^{2+} ions in place of Ni^{2+} ions, from 0.2 to 0.4 the Bragg's angle shifts towards lower angle and thereby interplaner spacing 'd' values increases. The Lattice constant and Particle size is found to increase with increase in Cu^{2+} doping from 0.2 to 0.4. The Lattice constant and Particle size is found to decrease for further doping of Cu^{2+} from 0.4 to 0.6, x.

The variations in lattice constant as a function of Copper concentration x can be understood on the basis of the ionic radius of the substituted cations. Since the ionic radius of Cu^{2+} ions (0.73Å) is greater than that of Ni^{2+} ions (0.69Å), the substitution is expected to increase the lattice constant with increase in Copper concentration x **[20-22]**. When the larger Copper ions enter, the lattice unit cell expands while preserving overall symmetry this is true as long as the lattice constant increases with substituent concentration of Copper. The values of Particle size and lattice constant obtained from XRD data by varying Cu^{2+} ions doping are given in **Table 6**. **Fig 11** and **Fig 13** show the correlation between Particle Size and Lattice Constant due to doping of Cu^{2+} ions.

3.5. AC conductivity (σ) at different concentration of Ni^{2+} ions (A, B and C)

The AC conductivity of all ferrite samples due to Ni^{2+} ions doping is calculated in the frequency range of 100 Hz to 5 MHz and average of AC conductivity if each sample is taken in to consideration for plotting the graph of Ni^{2+} ions doping (x=0.2,0.4 & 0.6) verses average AC conductivity. From **Fig. 4** it is observed that average AC conductivity decreases with increase of Ni^{2+} ions doping.

With the increase in the concentration of Ni^{2+} ions (x), the hopping action of charge carriers decreases due to the decreased concentration of Fe^{3+} ions at B-site. It is observed that Lattice constant, particle size and AC conductivity decreases with Ni^{2+} doping (x=0.2, 0.4 & 0.6). **Table 7** shows the average AC conductivity of ferrite samples A, B & C.

3.6. AC conductivity (σ) at different concentration of Co^{2+} ions (D, E and A)

The AC conductivity of all ferrite samples due to **Co^{2+}** doping is calculated in the frequency range of 100 Hz to 5 MHz and average of AC conductivity if each sample is taken in to consideration for plotting the graph of Co^{2+} doping (x=0.2,0.4 & 0.6) verses average AC conductivity. From **Fig. 8** it is observed that average AC conductivity increases with increase of **Co^{2+}**doping from 0.2 to 0.4 and thereafter AC conductivity decreases with increase of Co^{2+} doping from 0.4 to 0.6.

The decrease in AC conductivity may be due to effect of skin depth and decreases value of Cu^{2+} ions in SET-II. **Table 8** shows the average AC conductivity of ferrite samples D, E & A.

3.7. AC conductivity (σ) at different concentration of Cu^{2+} ions (C, F and D)

The AC conductivity of all ferrite samples due to Cu^{2+}**ions** doping is calculated in the frequency range of 100 Hz to 5 MHz and average of AC conductivity if each sample is taken in to consideration for plotting the

ISSN(Online) : 2319-8753
ISSN (Print) : 2347-6710

International Journal of Innovative Research in Science, Engineering and Technology

(An ISO 3297: 2007 Certified Organization)

Website: www.ijirset.com

Vol. 6, Issue 6, June 2017

graph of Cu^{2+} **ions** doping (x=0.2,0.4 & 0.6) verses average AC conductivity. From **Fig. 14** it is observed that average AC conductivity increases with increase of Cu^{2+} **ions** doping.

With the increase in the concentration of Cu^{2+} ions (x), the hopping action of charge carriers increases due to the increased concentration of Fe^{3+} ions at B-site.

It is well known that the mechanism of the electrical conduction is the same as that of the dielectric polarization **[23-24]. Table 9** shows the average AC conductivity of ferrite samples C, F & D.

The FTIR spectroscopy confirms the single phase nature of the prepared sample. The peak 536.114 cm $^{-1}$ gives the confirmation of Fe_2O_4. Fig. 8 shows the IR absorption peak at 536.114 cm $^{-1}$.

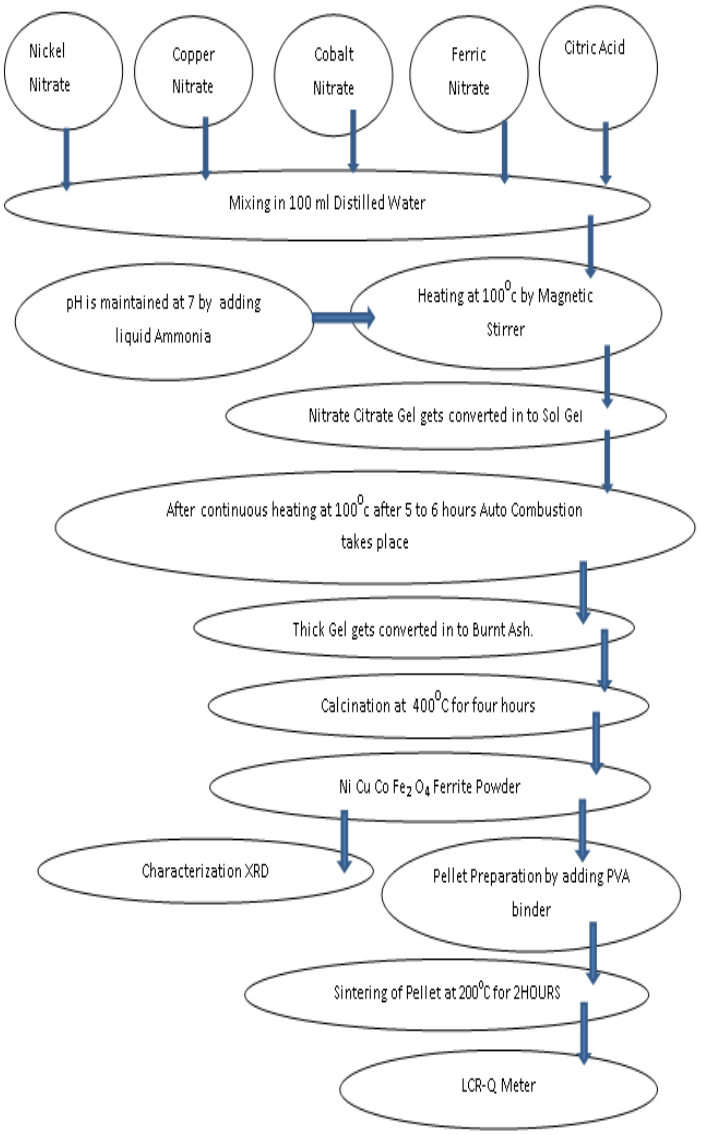

Fig.1: Flow Chart of SOL GEL for Ferrite Material and Pellet fabrication

ISSN(Online) : 2319-8753
ISSN (Print) : 2347-6710

International Journal of Innovative Research in Science, Engineering and Technology

(An ISO 3297: 2007 Certified Organization)

Website: www.ijirset.com

Vol. 6, Issue 6, June 2017

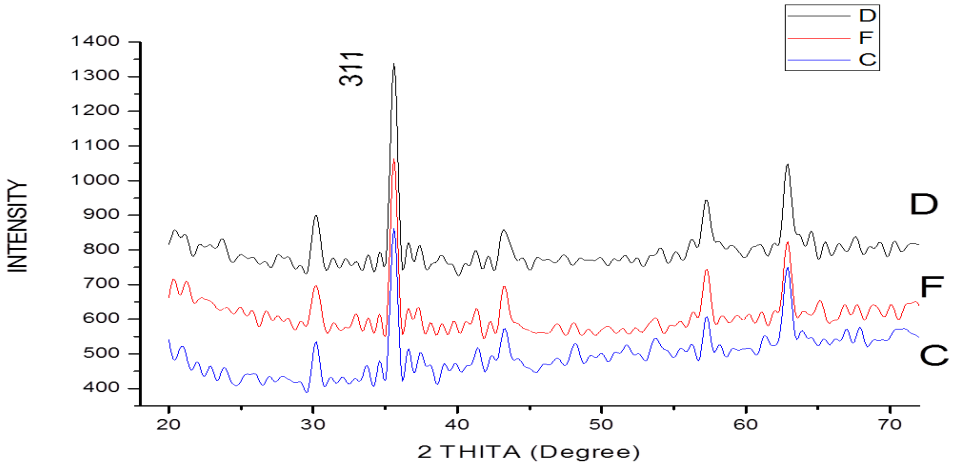

Fig. 2 XRD Pattern of SET-II ferrite samples.

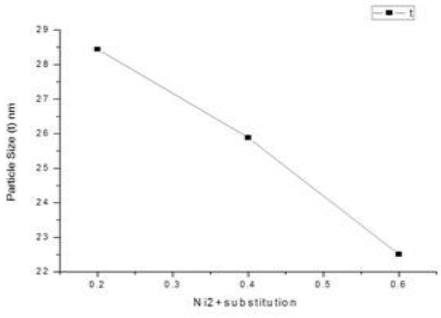

Fig. 3: Ni^{2+} doping verses particle size.

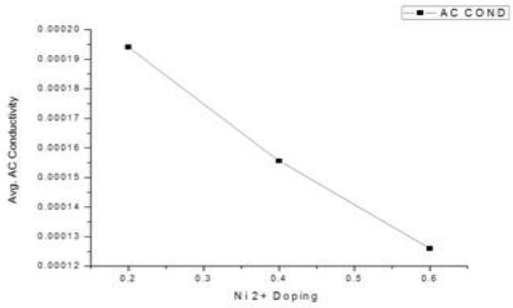

Fig. 4: Ni^{2+} doping verses Avg. AC Conductivity.

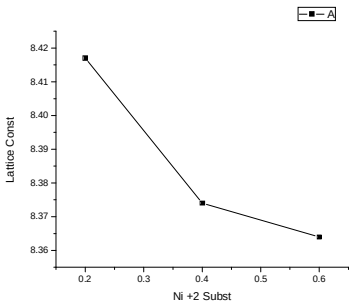

Fig 5: Ni^{2+}substitution verses Lattice Constant

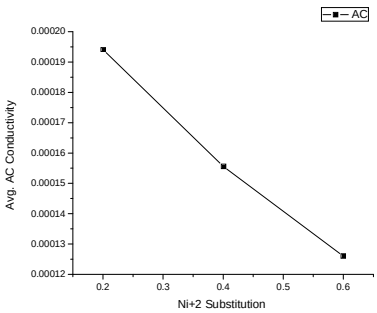

Fig 6: Ni^{2+}substitution verses Avg.AC Conductivity

ISSN(Online) : 2319-8753
ISSN (Print) : 2347-6710

International Journal of Innovative Research in Science, Engineering and Technology

(An ISO 3297: 2007 Certified Organization)

Website: www.ijirset.com

Vol. 6, Issue 6, June 2017

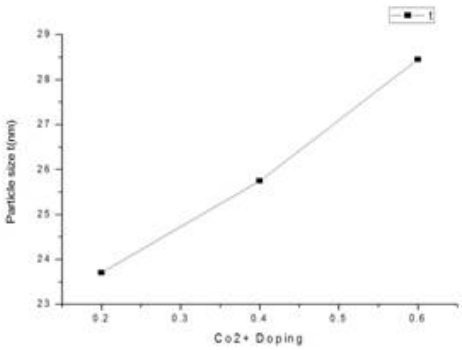

Fig. 7: Co^{2+} doping verses particle size.

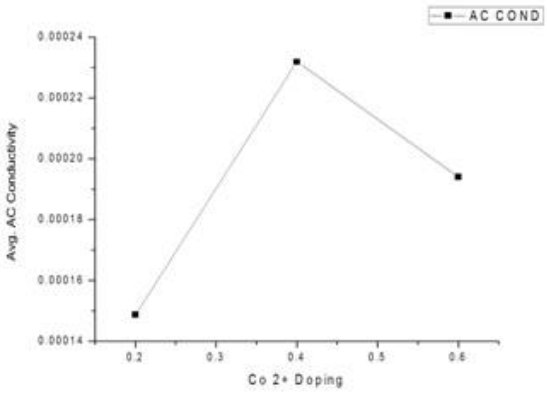

Fig. 8: Co^{2+} doping verses Avg. AC conductivity.

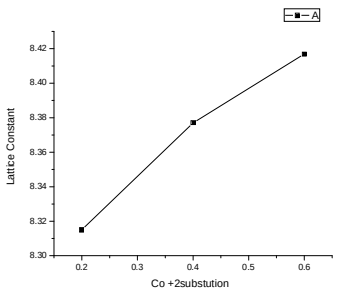

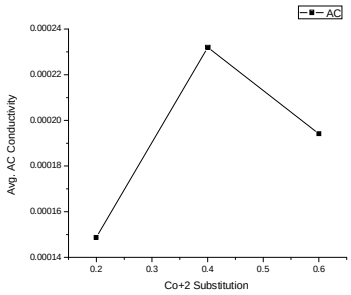

Fig 9: Co^{2+} substitution verses Lattice Constant Fig 10: Co^{2+} substitution verses Avg.AC Conductivity

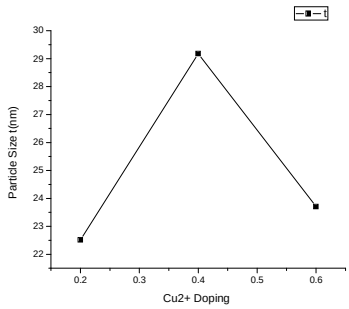

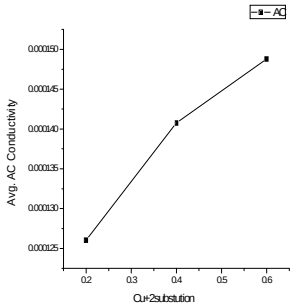

Fig 11: Cu^{2+} substitution verses Particle Size. Fig 12: Cu^{2+} substitution verses Avg. AC Conductivity

ISSN(Online) : 2319-8753
ISSN (Print) : 2347-6710

International Journal of Innovative Research in Science, Engineering and Technology

(An ISO 3297: 2007 Certified Organization)

Website: www.ijirset.com

Vol. 6, Issue 6, June 2017

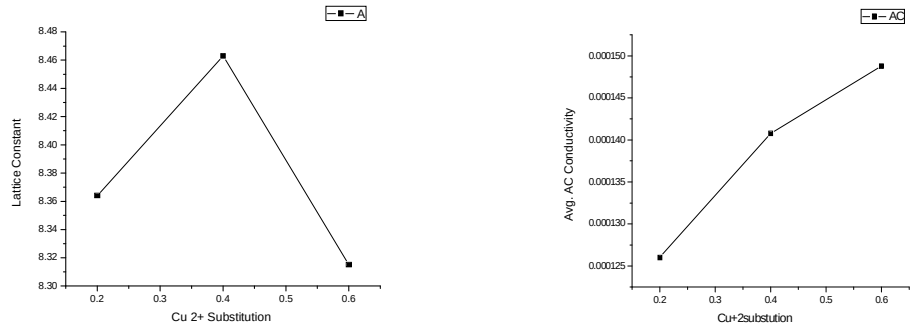

Fig 13: Cu^{2+}substitution verses Lattice Constant. Fig 14: Cu^{2+}substitution Verses Avg. AC Conductivity

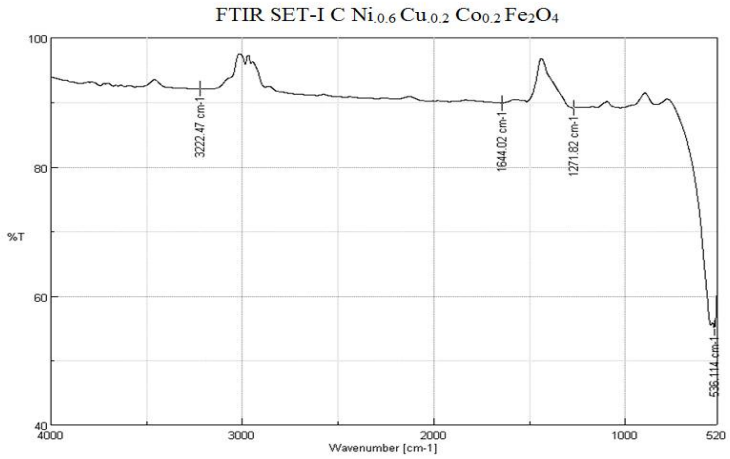

Fig 15: FTIR graph for SET-I (C)

Table 1: Label and Composition of Ferrite Material.

SET	Label	Ferrite Material
SET-I	A	$[(Ni_{.0.2}\,Cu_{.0.2}Co_{0.6})Fe_2O_4]$
	B	$[(Ni_{.0.4}\,Cu_{.0.2}Co_{0.4})Fe_2O_4]$
	C	$[(Ni_{.0.6}\,Cu_{.0.2}Co_{0.2})Fe_2O_4]$
SET-II	D	$[(Ni_{.0.2}\,Cu_{.0.6}\,Co_{0.2})Fe_2O_4]$
	E	$[(Ni_{.0.2}\,Cu_{.0.4}\,Co_{0.4})Fe_2O_4]$
	A	$[(Ni_{.0.2}\,Cu_{.0.2}\,Co_{0.6})Fe_2O_4]$
SET-III	C	$[(Ni_{.0.6}\,Cu_{.0.2}Co_{0.2})Fe_2O_4]$
	F	$[(Ni_{.0.4}\,Cu_{.0.4}Co_{0.2})Fe_2O_4]$
	D	$[(Ni_{.0.2}\,Cu_{.0.6}Co_{0.2})Fe_2O_4]$

ISSN(Online) : 2319-8753
ISSN (Print) : 2347-6710

International Journal of Innovative Research in Science, Engineering and Technology

(An ISO 3297: 2007 Certified Organization)

Website: www.ijirset.com

Vol. 6, Issue 6, June 2017

Table 2: Average AC Conductivity of Ferrite Samples (A to F).

Ferrite Material	Avg. AC Conductivity
SET-I- A $[(Ni_{0.2}Cu_{0.2}Co_{0.6})Fe_2O_4]$	0.000194143
SET-I- B $[(Ni_{0.4}Cu_{0.2}Co_{0.4})Fe_2O_4]$	0.000155638
SET-I- C $[(Ni_{0.6}Cu_{0.2}Co_{0.2})Fe_2O_4]$	0.000126047
SET-II- D $[(Ni_{0.2}Cu_{0.6}Co_{0.2})Fe_2O_4]$	0.000148797
SET-II- E $[(Ni_{0.2}Cu_{0.4}Co_{0.4})Fe_2O_4]$	0.000231988
SET-III- F $[(Ni_{0.4}Cu_{0.4}Co_{0.2})Fe_2O_4]$	0.000140762

Table 3: Particle Size and Lattice Constant of Ferrite Samples(A to F).

Ferrite Sample	Particle Size t (nm)	Lattices Constant (Å)
SET-I- A $[(Ni_{0.2}Cu_{0.2}Co_{0.6})Fe_2O_4]$	28.45	8.417
SET-I- B $[(Ni_{0.4}Cu_{0.2}Co_{0.4})Fe_2O_4]$	25.89	8.374
SET-I- C $[(Ni_{0.6}Cu_{0.2}Co_{0.2})Fe_2O_4]$	22.52	8.364
SET-II- D $[(Ni_{0.2}Cu_{0.6}Co_{0.2})Fe_2O_4]$	23.71	8.315
SET-II- E $[(Ni_{0.2}Cu_{0.4}Co_{0.4})Fe_2O_4]$	25.75	8.377
SET-III- F $[(Ni_{0.4}Cu_{0.4}Co_{0.2})Fe_2O_4]$	29.18	8.463

Table 4: Particle Size and Lattice Constant due to Ni^{2+} doping for SET-I Ferrite Samples.

Ferrite Sample	Particle Size t (nm)	Lattices Constant (Å)
SET-I- A $[(Ni_{0.2}Cu_{0.2}Co_{0.6})Fe_2O_4]$	28.45	8.417
SET-I- B $[(Ni_{0.4}Cu_{0.2}Co_{0.4})Fe_2O_4]$	25.89	8.374
SET-I- C $[(Ni_{0.6}Cu_{0.2}Co_{0.2})Fe_2O_4]$	22.52	8.364

Table 5: Particle Size and Lattice Constant due to Co^{2+} doping for SET-II Ferrite Samples.

Ferrite Sample	Particle Size t (nm)	Lattices Constant (Å)
SET-II- D $[(Ni_{0.2}Cu_{0.6}Co_{0.2})Fe_2O_4]$	23.71	8.315
SET-II- E $[(Ni_{0.2}Cu_{0.4}Co_{0.4})Fe_2O_4]$	25.75	8.377
SET-I- A $[(Ni_{0.2}Cu_{0.2}Co_{0.6})Fe_2O_4]$	28.45	8.417

Table 6: Particle Size and Lattice Constant due to Cu^{2+} doping for SET-III Ferrite Samples.

Ferrite Sample	Particle Size t (nm)	Lattices Constant (Å)
SET-I- C $[(Ni_{0.6}Cu_{0.2}Co_{0.2})Fe_2O_4]$	22.52	8.364
SET-III- F $[(Ni_{0.4}Cu_{0.4}Co_{0.2})Fe_2O_4]$	29.18	8.463
SET-II- D $[(Ni_{0.2}Cu_{0.6}Co_{0.2})Fe_2O_4]$	23.71	8.315

Table 7: Average AC Conductivity of SET-I.

$[Ni_xCu(constant)Co_{0.8-x}Fe_2O_4]$,Cu=constant=0.2	
x	Avg. AC Conductivity
(A) For x=0.2	0.000194143
(B) For x=0.4	0.000155638
(C) For x=0.6	0.000126047

ISSN(Online) : 2319-8753
ISSN (Print) : 2347-6710

International Journal of Innovative Research in Science, Engineering and Technology

(An ISO 3297: 2007 Certified Organization)

Website: www.ijirset.com

Vol. 6, Issue 6, June 2017

Table 8: Average AC Conductivity of SET-II.

$[(Ni_{(constant)}\ Cu_{0.8-x}Co_x)Fe_2O_4]$, Ni =constant=0.2	
x	Avg. AC Conductivity
(D) For x=0.2	0.000148797
(E) For x=0.4	0.000231988
(A) For x=0.6	0.000194143

Table 9: Average AC Conductivity of SET-III.

$[(Ni_{0.8-x}Cu_x\ Co_{(constant)})Fe_2O_4]$, Co = constant = 0.2	
x	Avg. AC Conductivity
(C) For x=0.2	0.000126047
(F) For x=0.4	0.000140762
(D) For x=0.6	0.000148797

IV. CONCLUSION

We have successfully prepared six different types of Nanocrystalline Ferrite materials by successfully implementing Sol Gel Auto combustion method. All ferrite materials are having particle size in nanometer range and exhibit good AC conductivity. Ferrite materials can use as core in transformer as well as fabricating antenna and as dielectric material in capacitors.

REFERENCES

[1] C. G. Whinfrey, D. W. Eckort and A. Tauber, *J. Am. Chem. Soc.* 53 (1982) 2722
[2] C. Caizer, M. Stefanescu, *J. Phys. D. Appl. Phys.*35 (2002) 3035
[3] M.A. Ahmed, S.F. Mansour, M. Afifi, *J. Magn. Magn. Mater*. 324 (2012) 4-10
[4] P.S. Aghav, V.N. Dhage, M.L. Mane, D.R. Shengule, R.G. Dorik, K.M. Jadhav, *Physica B: Cond. Matter*. 406(2011) 4350
[5] S. Sun, C.B. Murray, D. Weller, L. Folks, A. Moser, *Science 287* (2000) 1989
[6] I.H. Gul, W. Ahmed, A. Maqsood, *J. Magn. Magn. Mater*, 320 (2008) 270–275
[7] K. Byrappa, M. Yoshimura, Handbook of Hydrothermal Technology, Noyes Publications, New Jersey, USA, 2001.
[8] P. Hermankova, M. Hermanek, R. Zboril, Eur. J. Inorg. Chem., 2010, 1, 110.
[9] J. Moulder, Handbook of X-ray Photoelectron Spectroscopy (XPS), USA 1995.
[10] D. L. Pavla, G. L. Lampman, G. S. Krlz, J. R. Vyvyan, Introduction to spectroscopy, Brooks/ colecengage learning, 2009.
[11] K.W. Wagner, Ann. Phys. 40 (1913) 817.
[12] I.T. Rabinkin, Z.I. Novikova, Ferrites, Izv Acad. Nauk USSR, Minsk, 1960.
[13] J.C. Maxwell, Electricity and Magnetism, vol. 1, Oxford University Press, New York (1973), p. 1.
[14] M. Penchal Reddy, W. Madhuri, N. Ramamanoher Reddy, K.V. Siva Kumar, V.R.K. Murthy, R. Ramakrishna Reddy, Influence of copper substitution on magnetic and electrical properties of MgCuZn ferrite prepared by microwave sintering method, Mater. Sci. Eng. C 30 (2010) 1094–1099.
[15] K J. Azadmanjiri, H.K. Salehani, M.R. Barati, F. Farzan, Preparation and electromagnetic properties of Ni1 xCuxFe2O4 nanoparticle ferrites by sol–gel auto-combustion method, Mater. Lett. 61 (2007) 84–87.
[16] M.A. Ahmed, S.F. Mansour, M. Afifi, J. Magn. Magn. Mater. 324 (2012) 4-10.
[17] P.S. Aghav, V.N. Dhage, M.L. Mane, D.R. Shengule, R.G. Dorik, K.M. Jadhav, Physica B: Cond. Matter. 406(2011) 4350.
[18] J. Jing, L. Liangchao, X. Feng, J. Rare Earths 25 (2007) 79.
[19] J. Azadmanjiri, H.K. Salehani, M.R. Barati, F. Farzan, *Mater. Lett.* 61 (2007) 84–87.
[20] J. Du, Z. Liu, W. Wu, Z. Li, B. Han, Y. Huang, *Mater. Res. Bull.* 40 (2005) 928–935.
[21] M.R. Anantharaman, S. Sindhu, S. Jagatheesan, K.A. Malini, P. Kurian, J Phys. D 32 (1999) 1801
[22] T. Nakamura, Y. Okaro, Electromagnetic properties of Mn–Zn ferrite sintered ceramics, *J. Appl. Phys.* 79 (1996) 7129.
[23] T. Jahanbin, M. Hashim, K. A. Mantori, J. Magn. Magn. Mater. 322(2010) 2684-2689.
[24] G.F. Goya, H.R. Rechenberg, Superparamagnetic transition and local-order in $CuFe_2O_4$ nanoparticles, Nanostruct. Mater. 10 (1998) 1001–1011.